

Dissociation of quarkonium in a complex potential

Lata Thakur, Uttam Kakade, and Binoy Krishna Patra

Department of Physics, Indian Institute of Technology Roorkee, Roorkee 247 667 Uttarakhand, India

(Received 1 January 2014; published 23 May 2014)

We have studied the quasifree dissociation of quarkonia through a complex potential that is obtained by correcting both the perturbative and nonperturbative terms of the Cornell potential through the dielectric function in real-time formalism. The real-part of the potential becomes stronger and thus makes the quarkonia more bounded, whereas the (magnitude) imaginary part too becomes larger and thus contributes more to the thermal width, compared to the medium contribution of the Coulomb term alone. These cumulative effects result in the quarkonia dissociating at higher temperatures. Finally, we extend our calculation to a medium, exhibiting local momentum anisotropy, by calculating the leading anisotropic corrections to the propagators in Keldysh representation. The presence of anisotropy makes the real part of the potential stronger but the imaginary part is weakened slightly. However, since the medium correction to the imaginary part is a small perturbation to the vacuum part, overall the anisotropy makes the dissociation temperatures higher, compared to the isotropic medium.

DOI: [10.1103/PhysRevD.89.094020](https://doi.org/10.1103/PhysRevD.89.094020)

PACS numbers: 12.39.-x, 11.10.St, 12.38.Mh, 12.39.Pn

I. INTRODUCTION

The study of the heavy quarkonium states at finite temperature got impetus after the proposal by Matsui and Satz [1] where the dissociation of quarkonium due to the color screening in the deconfined medium signals the formation of quark-gluon plasma (QGP) [2]. The assumption behind the proposal is that the medium effects can be envisaged through temperature-dependent heavy quark potentials and they have been studied over the decades either phenomenologically or through lattice based free-energy calculations [3,4]. In recent years there have been important theoretical developments in heavy quarkonium physics where a sequence of effective field theories (EFT) [5–9] is derived by exploiting the hierarchy of different scales of the heavy quark bound state, $m_Q \gg m_Q v \gg m_Q v^2$, due to its large quark mass (m_Q). For example, the heavy quark system can be described by nonrelativistic quantum chromodynamics (NRQCD) obtained from QCD by integrating out the mass. To describe the bound state of two quarks, one can further integrate out the typical momentum exchange ($m_Q v$) between the bound quarks [5,6] and this leads to potential nonrelativistic QCD (pNRQCD), which describes a bound state by a two point function satisfying the Schrödinger equation through the potentials as the matching coefficients of the Lagrangian. The EFT can also be generalized to finite temperature to justify the use of potential models at finite temperature [10], but the thermal scales (T , gT , etc.) make the analysis complicated. For example, when the binding energy is larger than the temperature, there are no medium modifications of the heavy quark potential [10], but the properties of quarkonia states will be affected through the interactions with ultrasoft gluons. As a result, the binding energy gets reduced and a finite thermal width is developed

due to the medium induced singlet-octet transitions arising from the dipole interactions [10]. This temperature regime is relevant for the $\Upsilon(1S)$ suppression at the LHC. In the opposite limit (the binding energy $< T < gT$), the potential acquires an imaginary component [10]. However, beyond the leading order, the above distinctions are no longer possible.

In non-EFT, the heavy quark potential is defined from the late-time behavior of the Wilson loop [11,12] and can be directly calculated either in Euclidean-time lattice simulations or in perturbation theory [13]. However, the definition of the heavy quark potential related to the finite-temperature real-time Wilson loop, as employed in the lattice QCD extraction, is also based on an application of EFT [14,15], where the derivation proceeds on the level of NRQCD and happens to be complex [10,16]. The imaginary part of the potential can be interpreted as the Landau damping [17] that describes the decaying of the $Q\bar{Q}$ correlation with its initial state due to scatterings in the plasma.

The separation of thermal scales in EFT ($T \gg gT \gg g^2 T$) (in the weak-coupling regime) in practice is not evident and one needs lattice techniques to test the approach. To understand the color screening in the strong-coupling regime, lattice calculations of the spatial correlation functions of static quarks are needed. In principle, it is possible to study the problem of quarkonium dissolution without any use of potential models. Recently, a lot of progress has been made in this direction in which the in-medium properties of different quarkonium states are encoded in spectral functions in terms of the Euclidean meson correlation functions constructed on the lattice [18–26]. However, the reconstruction of the spectral functions from the lattice meson correlators turns out to be very difficult, and despite several attempts its outcome

still remains inconclusive. One remarkable feature of the studies of the lattice meson correlators is their feeble temperature dependence despite the expected color screening. This seems puzzling.

Not only is the determination of the effective potential still an open question but there are also other related issues such as relativistic effects, thermal width of the states, and contribution from quantum corrections that need to be taken care of. The physical picture of quarkonium dissociation in a medium has undergone theoretical refinements over the last couple of years [27,28]. Experimentally, the properties of thermally produced heavy quarkonium can be observed through the energy spectrum of their decay products (the dilepton pair) [29,30]. The dissociation of quarkonium resonances corresponds to the disappearance of their peaks in the dilepton production rate. However, merely estimating the energy levels from the potential models does not allow one to reconstruct the spectral function, which can determine the production rate [31]. Physically, a resonance dissolves into a medium through the broadening of its peak gradually, due to its interaction with the partons in the medium. Earlier it was thought that a quarkonium state is dissociated when the Debye screening becomes so strong that it inhibits the formation of bound states, but nowadays a quarkonium is dissociated at a lower temperature [16,31] even though its binding energy is nonvanishing; rather it is overtaken by the Landau-damping induced thermal width [32], obtained from the imaginary part of the potential. Its consequences on heavy quarkonium spectral functions [31,33], perturbative thermal widths [32,34], quarkonia at finite velocity [35], in a T-matrix approach [36–40], and in stochastic real-time dynamics [41] have been studied. Recently, the dynamical evolution of the plasma was combined with the real and imaginary parts of the binding energies to estimate the suppression of quarkonium [42] in RHIC and LHC energies.

As discussed above, in-medium corrections to the potential are always accompanied by both real and imaginary components. In the weak-coupling regime, the Landau damping caused by the imaginary component is the principle mechanism for the dissociation of heavy quark bound states. Hence, any realistic calculation of the spectral functions needs to incorporate both of the real and imaginary parts. However, the separation of the scales, which are related to the screening of static electric fields (gT) and magnetic fields (g^2T) etc., are not satisfied at the strong-coupling limit and thus needs to handle nonperturbatively through the lattice studies. Although the lattice studies have shown that a sizable imaginary component is visible in the potential [43,44], they may not be reliable because the necessary quality of the data has not yet been achieved. One thus needs inadvertent support from the potential models at finite temperature as an important tool to complement the lattice studies.

Usually potential model studies are limited to the medium modification of the perturbative part of the potential only. It is found that the bulk properties of the QCD plasma phase, e.g., the screening property, equation of state [45,46], etc., deviate from the perturbative predictions, even beyond the deconfinement temperature. In the sequel, the phase transition in QCD for physical quark masses is found to be a crossover [47,48]. It is thus reasonable to assume that the string tension does not vanish abruptly at the deconfinement point [49–51], so one should study its effects on heavy quark potential even above T_c . This issue, usually overlooked in the literature where only a screened Coulomb potential was assumed above T_c and the linear/string term was neglected, was certainly worth investigation. Sometimes a one-dimensional Fourier transform of the Cornell potential was employed with the assumption of a color flux tube [52] in one dimension but at finite temperature; it may not be the case since the flux tube structure may expand in more dimensions [53]. Therefore, it would be better to consider the three-dimensional form of the medium modified Cornell potential. Recently, a heavy quark potential was obtained by correcting both perturbative and nonperturbative terms in the Cornell potential, not its Coulomb part alone, with a dielectric function encoding the effects of the deconfined medium [54]. The inclusion of the nonvanishing string term, apart from the Coulomb term, made the potential more attractive, which can be seen by an additional long-range Coulomb term, in addition to the conventional Yukawa term. In the short-distance limit, the potential reduces to the vacuum one, i.e., the $Q\bar{Q}$ pair does not see the medium, whereas in the long-distance limit, potential reduces to a long-range Coulomb potential with a dynamically screened-color charge. Thereafter with this potential, the binding energies and dissociation temperatures of the ground and the lowest-lying states of charmonium and bottomonium spectra have been determined [54,55].

The discussions on the medium modifications of quarkonium properties referred to above are restricted to the isotropic medium only; it was until recently that the effect of anisotropy was considered in the heavy-ion collisions [56]. At the very early time of collision, asymptotic weak coupling enhances the longitudinal expansion more substantially than the radial expansion; thus, the system becomes colder in the longitudinal direction than in the transverse direction and causes an anisotropy in the momentum space. The anisotropy thus generated affects the evolution of the system as well as the properties of quarkonium states. In recent years, the effects of anisotropy on both real and imaginary parts of the heavy quark potential and subsequently on the dissociation of quarkonia states have been investigated in an anisotropic medium [57–61] extensively. Recently, we extended our aforesaid calculation [54] for an isotropic medium to a medium that exhibits a local anisotropy in the momentum space by correcting the full Cornell potential through the hard-loop

resumed gluon propagator [62]. The presence of anisotropy introduces an angular dependence, in addition to interparticle separation, to the potential that is manifested in weakening the screening of the potential. As a result, the resonances become more bound than in the isotropic medium. Since the weak anisotropy represents a perturbation to the (isotropic) spherical potential, we obtained the first-order correction due to the small anisotropic contribution to the energy eigenvalues of the spherically symmetric potential and explored how the properties of quarkonium states change in the anisotropic medium. For example, the dissociation temperatures are found to be minimum for the isotropic case and increase with the increase of anisotropy.

In the present work we aim to calculate the imaginary part, in addition to the real part of the potential both in the isotropic and anisotropic medium, by correcting the full Cornell potential, not its Coulomb part alone. Therefore, we first revisit the leading anisotropic corrections to the real and imaginary parts of the retarded, advanced, and symmetric propagators through their self energies, and then plug in their static limit to evaluate the real and imaginary part of the static potential, respectively. This imaginary part provides a contribution to the width (Γ) of quarkonium bound states [16,17,32], which in turn determines their dissociation temperatures by the criterion: the dissociation point of a particular resonance is defined as the temperature where twice the (real part of) binding energy equals to Γ [23,31,63,64] or from the intersection of the real and imaginary parts of the binding energies. The structure of our paper is as follows. Section II is devoted to the formalism of the potential in both isotropic and anisotropic mediums. So we have started with a review of the retarded, advanced, and symmetric propagators and self energies in Keldysh representation and their evaluation in hard thermal loop (HTL) resummed theory in both isotropic and anisotropic mediums in Sec. II A. With these ingredients, we calculated the real and imaginary parts of the (static) potential and subsequently studied the dissociation of charmonium and bottomonium states by calculating their real and imaginary binding energies and (thermal) widths for isotropic and anisotropic medium in subsection II B and II C, respectively. Moreover, we show our results and try to explain them in terms of various effects: the contribution of the nonperturbative (string) term, the anisotropy, the screening scale, etc. Finally, we conclude our main results in Sec. III.

II. POTENTIAL IN A HOT QCD MEDIUM

As discussed earlier, any meaningful discussion of quarkonium properties in the thermal medium should include both real and imaginary parts for the temperature-dependent potential. The hierarchy of scales assumed in weak-coupling EFT calculations may not be satisfied and adequate quality of the data is not available in the present lattice calculations, so one uses the potential model to circumvent the problem.

Because of the heavy quark mass (m_Q), the requirement $m_Q \gg \Lambda_{QCD}$ and $T \ll m_Q$ is satisfied for the description of the interactions between a pair of heavy quarks and antiquarks at finite temperature, in terms of quantum mechanical potential. So we can obtain the medium modification to the vacuum potential by correcting its both short and long-distance part with a dielectric function $\epsilon(p)$ encoding the effect of deconfinement [54]:

$$V(r, T) = \int \frac{d^3 \mathbf{p}}{(2\pi)^{3/2}} (e^{i\mathbf{p}\cdot\mathbf{r}} - 1) \frac{V(p)}{\epsilon(p)}, \quad (1)$$

where we have subtracted an r -independent term (to renormalize the heavy quark free energy), which is the perturbative free energy of quarkonium at infinite separation [65]. The functions, $V(p)$ and $\epsilon(p)$, are the Fourier transforms (FT) of the Cornell potential and the dielectric permittivity, respectively. To obtain the FT of the potential, we regulate both terms with the same screening scale. However, in the framework of Debye-Hückel theory, Digal *et al.* [66] employed different screening functions, f_c and f_s , for the Coulomb and string terms, respectively, to obtain the free energy.¹

At present, we regulate both terms by multiplying with an exponential damping factor that is switched off after the FT is evaluated. This has been implemented by assuming r as the distribution ($r \rightarrow r \exp(-\gamma r)$). The FT of the linear part $\sigma r \exp(-\gamma r)$ is

$$-\frac{i}{p\sqrt{2\pi}} \left(\frac{2}{(\gamma - ip)^3} - \frac{2}{(\gamma + ip)^3} \right). \quad (2)$$

After putting $\gamma = 0$, we obtain the FT of the linear term σr as

$$(\tilde{\sigma r}) = -\frac{4\sigma}{p^4\sqrt{2\pi}}. \quad (3)$$

The FT of the Coulomb piece is straightforward; thus, the FT of the full Cornell potential becomes

$$V(p) = -\sqrt{(2/\pi)} \frac{\alpha}{p^2} - \frac{4\sigma}{\sqrt{2\pi}p^4}. \quad (4)$$

The dielectric permittivity will be calculated once the self energies and propagators are obtained in HTL resummation theory.

A. HTL SELF ENERGIES AND PROPAGATORS

The naive perturbative expansion, when applied to gauge fields, suffers from various singularities and even the damping rate becomes gauge dependent [69]. Diagrams

¹In another calculation, different scales for the Coulomb and linear pieces were also employed in [67,68] to include non-perturbative effects in the free energy beyond the deconfinement temperature through a dimension-two gluon condensate.

that are of higher order in the coupling constant (g) contribute to the leading order. These problems can be partly avoided by using the HTL resummation technique [70] to obtain the consistent results, which are complete to the leading order. At the same time, the infrared behavior is improved by the presence of effective masses in the HTL propagators. The HTL technique has been shown to be equivalent to the transport approach [71,72] and is more advantageous because it can be naturally extended to fermionic self energies and to higher-order diagrams beyond the semiclassical approximation.

We shall now calculate the finite temperature self energies and propagator in real-time formalism [73] where the propagators acquire a 2×2 matrix structure,

$$D^0 = \begin{pmatrix} D_{11}^0 & D_{12}^0 \\ D_{21}^0 & D_{22}^0 \end{pmatrix}, \quad (5)$$

where each component has zero and finite temperature parts that contain the distribution functions. In equilibrium, the distribution functions correspond to either (isotropic) Bose (f_B) or Fermi distribution (f_F) functions. Away from the equilibrium, the distribution function needs to be replaced by the corresponding nonequilibrium one extracted from viscous hydrodynamics. The nonequilibrium situation arises due to preferential expansion and nonzero viscosity and, as a consequence, a local anisotropy in momentum space sets in. However, we consider a system close to equilibrium where the distribution function can be obtained from an isotropic one by removing particles with a large momentum component along the direction of anisotropy [56,74], \mathbf{n} , i.e.,

$$f_{\text{aniso}}(\mathbf{p}) = f_{\text{iso}}(\sqrt{\mathbf{p}^2 + \xi(\mathbf{p} \cdot \mathbf{n})^2}) \\ \approx f_{\text{iso}}(p) \left[1 - \xi \frac{(\mathbf{p} \cdot \mathbf{n})^2}{2pT} (1 \pm f_{\text{iso}}(p)) \right]. \quad (6)$$

The anisotropic parameter ξ is related to the shear viscosity-to-entropy density (η/s) through the one-dimensional Navier Stokes formula by

$$\xi = \frac{10\eta}{T\tau s}, \quad (7)$$

where $1/\tau$ denotes the expansion rate of the fluid element. The degree of anisotropy is generically defined by

$$\xi = \frac{\langle \mathbf{k}_T^2 \rangle}{2\langle k_L^2 \rangle} - 1, \quad (8)$$

where $k_L = \mathbf{k} \cdot \mathbf{n}$ and $\mathbf{k}_T = \mathbf{k} - \mathbf{n}(\mathbf{k} \cdot \mathbf{n})$ are the components of momentum parallel and perpendicular to the direction of anisotropy, \mathbf{n} , respectively. The positive and negative values of ξ correspond to the squeezing and stretching of

the distribution function in the direction of anisotropy, respectively. However, in relativistic nucleus-nucleus collisions, ξ is found to be positive. A useful representation of the propagators in real-time formalism is the Keldysh representation where the linear combinations of four components of the matrix, of which only three are independent, give the relation for the retarded (R), advanced (A), and symmetric (F) propagators, respectively:

$$D_R^0 = D_{11}^0 - D_{12}^0, \quad D_A^0 = D_{11}^0 - D_{21}^0, \\ D_F^0 = D_{11}^0 + D_{22}^0. \quad (9)$$

Only the symmetric component involves the distribution functions and is of particular advantage for the HTL diagrams where the terms containing distribution functions dominate. The similar relations for the self energies are

$$\Pi_R = \Pi_{11} + \Pi_{12}, \quad \Pi_A = \Pi_{11} + \Pi_{21}, \\ \Pi_F = \Pi_{11} + \Pi_{22}. \quad (10)$$

Resumming the propagators through the Dyson-Schwinger equation, the retarded (advanced) and symmetric propagators can be written as

$$D_{R,A} = D_{R,A}^0 + D_{R,A}^0 \Pi_{R,A} D_{R,A}, \quad (11)$$

$$D_F = D_F^0 + D_R^0 \Pi_R D_F + D_F^0 \Pi_A D_A + D_R^0 \Pi_F D_A. \quad (12)$$

Substituting the symmetric propagator $D_F^0(P)$ in terms of the retarded and advanced propagator, the resummed symmetric propagator can be expressed as

$$D_F(P) = (1 + 2f_B) \text{sgn}(p_0) [D_R(P) - D_A(P)] \\ + D_R(P) [\Pi_F(P) - (1 + 2f_B) \text{sgn}(p_0) [\Pi_R(P) \\ - \Pi_A(P)]] D_A(P). \quad (13)$$

To calculate the static potential in the isotropic medium, only the temporal component (L) of the propagator is needed so the retarded (advanced) propagator in the simplest Coulomb gauge can be written as

$$D_{R,A}^L(\text{iso}) = D_{R,A}^{L(0)} + D_{R,A}^{L(0)} \Pi_{R,A}^L(\text{iso}) D_{R,A}^L(\text{iso}). \quad (14)$$

So far the resummation is done in the isotropic medium; however, we now extend it in a medium that exhibits a weak anisotropy ($\xi \ll 1$). Therefore, we first expand the propagators and self energies around the isotropic limit and retain only the linear term:

$$D = D_{\text{iso}} + \xi D_{\text{aniso}}, \quad \Pi = \Pi_{\text{iso}} + \xi \Pi_{\text{aniso}}. \quad (15)$$

Thus, in the presence of small anisotropy, the temporal component of the retarded (advanced) propagator becomes

$$D_{R,A(\text{aniso})}^L = D_{R,A}^{L(0)} \Pi_{R,A(\text{aniso})}^L D_{R,A(\text{iso})}^L + D_{R,A}^{L(0)} \Pi_{R,A(\text{iso})}^L D_{R,A(\text{aniso})}^L, \quad (16)$$

whereas with the notations for the difference of propagators and self energies $\Delta D_{RA(\text{aniso})}^L = [D_{R(\text{aniso})}^L(P) - D_{A(\text{aniso})}^L(P)]$, $\Delta D_{RA(\text{iso})}^L = [D_{R(\text{iso})}^L(P) - D_{A(\text{iso})}^L(P)]$, $\Delta \Pi_{RA(\text{aniso})}^L = [\Pi_{R(\text{aniso})}^L(P) - \Pi_{A(\text{aniso})}^L(P)]$, and $\Delta \Pi_{RA(\text{iso})}^L = [\Pi_{R(\text{iso})}^L(P) - \Pi_{A(\text{iso})}^L(P)]$, the symmetric propagator can be obtained [65]:

$$D_{F(\text{aniso})}^L(P) = (1 + 2f_{B(\text{iso})}) \text{sgn}(p_0) \Delta_{RA(\text{aniso})}^L + 2f_{B(\text{aniso})} \text{sgn}(p_0) \Delta_{RA(\text{iso})}^L + D_{R(\text{iso})}^L(P) [\Pi_{F(\text{aniso})}^L(P) - (1 + 2f_{B(\text{iso})}) \text{sgn}(p_0) \Delta \Pi_{RA(\text{aniso})}^L - 2f_{B(\text{aniso})} \text{sgn}(p_0) \Delta \Pi_{RA(\text{iso})}^L] D_{A(\text{iso})}^L(P). \quad (17)$$

To solve the propagators, we will now calculate the gluon self energy from the quark and gluon loops. The contribution of the quark loop [65] to the self energy with external and internal momenta as $P(p_0, \mathbf{p})$ and $K(k_0, \mathbf{k})$, respectively (with $Q = K - P$),

$$\Pi^{\mu\nu}(P) = -\frac{i}{2} N_f g^2 \int \frac{d^4 K}{(2\pi)^4} \text{tr}[\gamma^\mu S(Q) \gamma^\nu S(K)], \quad (18)$$

gives the retarded self energy

$$\Pi_R^{\mu\nu}(P) = -\frac{i}{2} N_f g^2 \int \frac{d^4 K}{(2\pi)^4} (\text{tr}[\gamma^\mu S_{11}(Q) \gamma^\nu S_{11}(K)] - \text{tr}[\gamma^\mu S_{21}(Q) \gamma^\nu S_{12}(K)]). \quad (19)$$

Redefining the fermionic propagators, $S_{R,A,F}(K) \equiv K \tilde{\Delta}_{R,A,F}(K)$, the longitudinal part of the self energy becomes, in the limit of massless quarks,

$$\begin{aligned} \Pi_R^L(P) &= -i N_f g^2 \int \frac{d^4 K}{(2\pi)^4} (q_0 k_0 + \mathbf{q} \cdot \mathbf{k}) \\ &\quad \times [\tilde{\Delta}_F(Q) \tilde{\Delta}_R(K) + \tilde{\Delta}_A(Q) \tilde{\Delta}_F(K) \\ &\quad + \tilde{\Delta}_A(Q) \tilde{\Delta}_A(K) + \tilde{\Delta}_R(Q) \tilde{\Delta}_R(K)]. \quad (20) \end{aligned}$$

In the weak-coupling limit, the internal momentum (T) is much larger than the external momentum (gT), so the retarded self energy in the HTL approximation simplifies into [65]

$$\Pi_R^L(P) = \frac{4\pi N_f g^2}{(2\pi)^4} \int k dk \int d\Omega f_F(\mathbf{k}) \frac{1 - (\hat{\mathbf{k}} \cdot \hat{\mathbf{p}})^2}{(\hat{k} \cdot \hat{p} + \frac{p_0 + i\epsilon}{p})^2}. \quad (21)$$

After convoluting the distribution function, f_F for quarks in an (weakly) anisotropic medium from (6) the retarded quark self energy becomes

$$\Pi_R^L(P) = \frac{g^2}{2\pi^2} N_f \sum_{i=0,1} \int_0^\infty k \Phi_{(i)}(k) dk \int_{-1}^1 \Psi_{(i)}(s) ds, \quad (22)$$

with

$$\begin{aligned} \Phi_{(0)}(k) &= n_F(k), \\ \Phi_{(1)}(k) &= -\xi n_F^2(k) \frac{ke^{k/T}}{2T}, \\ \Psi_{(0)}(s) &= \frac{1 - s^2}{(s + \frac{p_0 + i\epsilon}{p})^2}, \\ \Psi_{(1)}(s) &= \cos^2 \theta_p \frac{s^2(1 - s^2)}{(s + \frac{p_0 + i\epsilon}{p})^2} + \frac{\sin^2 \theta_p}{2} \frac{(1 - s^2)^2}{(s + \frac{p_0 + i\epsilon}{p})^2}. \quad (23) \end{aligned}$$

Here, the angle (θ_p) is between \mathbf{n} and \mathbf{p} and $s \equiv \hat{\mathbf{k}} \cdot \hat{\mathbf{p}}$. After decomposing into isotropic ($\xi = 0$) and anisotropic ($\xi \neq 0$) pieces, the isotropic and anisotropic terms become

$$\Pi_{R(\text{iso})}^L(P) = N_f \frac{g^2 T^2}{6} \left(\frac{p_0}{2p} \ln \frac{p_0 + p + i\epsilon}{p_0 - p + i\epsilon} - 1 \right) \quad (24)$$

$$\begin{aligned} \Pi_{R(\text{aniso})}^L(P) &= N_f \frac{g^2 T^2}{6} \left(\frac{1}{6} + \frac{\cos 2\theta_p}{2} \right) + \Pi_{R(\text{iso})}^L(P) \\ &\quad \times \left(\cos 2\theta_p - \frac{p_0^2}{2p^2} (1 + 3 \cos 2\theta_p) \right), \quad (25) \end{aligned}$$

respectively. In the HTL limit, the structure of the gluon-loop contribution is the same as the quark loop, apart from the degeneracy factor and distribution function, so the quark and gluon loops together give the isotropic part of retarded (advanced) self energy,

$$\Pi_{R,A(\text{iso})}^L(P) = m_D^2 \left(\frac{p_0}{2p} \ln \frac{p_0 + p \pm i\epsilon}{p_0 - p \pm i\epsilon} - 1 \right), \quad (26)$$

with the prescriptions $+i\epsilon$ ($-i\epsilon$), for the retarded (advanced) self energies, respectively, whereas the anisotropic part for the retarded (advanced) self energies are

$$\begin{aligned} \Pi_{R,A(\text{aniso})}^L(P) &= \frac{m_D^2}{6} \left(1 + \frac{3}{2} \cos 2\theta_p \right) + \Pi_{R(\text{iso})}^L(P) \\ &\quad \times \left(\cos(2\theta_p) - \frac{p_0^2}{2p^2} (1 + 3 \cos 2\theta_p) \right), \quad (27) \end{aligned}$$

where $m_D^2 (= \frac{g^2 T^2}{6} (N_f + 2N_c))$ is the square of the Debye mass.

Similarly, the isotropic and anisotropic terms for the temporal component of the symmetric part are given by

$$\begin{aligned}\Pi_{F(\text{iso})}^L(P) &= -2\pi i m_D^2 \frac{T}{p} \Theta(p^2 - p_0^2), \\ \Pi_{F(\text{aniso})}^L(P) &= \frac{3}{2} \pi i m_D^2 \frac{T}{p} \\ &\quad \times \left(\sin^2 \theta_p + \frac{p_0^2}{p^2} (3 \cos^2 \theta_p - 1) \right) \Theta(p^2 - p_0^2).\end{aligned}\quad (28)$$

Thus, the gluon self energy is found to have both real and imaginary parts that are responsible for the Debye screening and the Landau damping, respectively, where the former is usually obtained from the retarded and advanced self energy and the later is obtained from the symmetric self energy alone.

So, to evaluate the real part of the static potential, the real part of the temporal component of the retarded (or advanced) propagator (in the static limit) is needed,

$$\begin{aligned}\text{Re}D_{R,A}^{00}(0, p) &= -\frac{1}{(p^2 + m_D^2)} \\ &\quad + \xi \frac{m_D^2}{6(p^2 + m_D^2)^2} (3 \cos 2\theta_p - 1),\end{aligned}\quad (29)$$

while for the imaginary part of the potential, the imaginary part of the temporal component of symmetric propagator is given by

$$\begin{aligned}\text{Im}D_F^{00}(0, p) &= \frac{-2\pi T m_D^2}{p(p^2 + m_D^2)^2} + \xi \left(\frac{3\pi T m_D^2}{2p(p^2 + m_D^2)^2} \sin^2 \theta_p \right. \\ &\quad \left. - \frac{4\pi T m_D^4}{p(p^2 + m_D^2)^3} \left(\sin^2 \theta_p - \frac{1}{3} \right) \right).\end{aligned}\quad (30)$$

With these real and imaginary parts of the self energies and propagators, we will obtain the (complex) potential in subsection(s) IIB and IIC for the isotropic and anisotropic medium, respectively.

B. POTENTIAL IN THE ISOTROPIC MEDIUM

1. Real part of the potential

The real part of the static potential can thus be obtained from Eq. (1) by substituting the dielectric permittivity $\epsilon(p)$ in terms of the physical “11” component of the gluon propagator. The relation between the dielectric permittivity and the static limit of the “00” component of the gluon propagator in the Coulomb gauge is obtained from the linear response theory:

$$\epsilon^{-1}(p) = -\lim_{\omega \rightarrow 0} p^2 D_{11}^{00}(\omega, p), \quad (31)$$

where the propagator D_{11}^{00} can be separated into real and imaginary parts as

$$D_{11}^{00}(\omega, p) = \text{Re}D_{11}^{00}(\omega, p) + \text{Im}D_{11}^{00}(\omega, p). \quad (32)$$

The real and imaginary parts can be further recast in terms of retarded/advanced and symmetric parts, respectively:

$$\begin{aligned}\text{Re}D_{11}^{00}(\omega, p) &= \frac{1}{2} (D_R^{00} + D_A^{00}) \quad \text{and} \\ \text{Im}D_{11}^{00}(\omega, p) &= \frac{1}{2} D_F^{00}.\end{aligned}\quad (33)$$

Thus, using the real part of retarded (advanced) propagator in the isotropic medium

$$\text{Re}D_{R,A}^{00}(0, p) = -\frac{1}{(p^2 + m_D^2)}, \quad (34)$$

the real part of the dielectric permittivity (also given in [75–77]) becomes

$$\epsilon(p) = \left(1 + \frac{m_D^2}{p^2} \right). \quad (35)$$

Note that this one-loop result in the linear response theory is a perturbative one, where the linear approximation in QCD holds as long as the mean-field four potential (A_μ^a) is much smaller than the temperature [78]. Actually, for the soft scales, the mean-field four potential is at the order of \sqrt{gT} and the linear approximation holds in the weak-coupling limit.

However, if one assumes that nonperturbative effects such as the string tension survive even much above the deconfinement point, then the dependence of the dielectric function on the Debye mass may get modified. So there is a caveat about the validity of the linear dependence of the dielectric function (ϵ) on the square of the Debye mass m_D^2 . For the sake of simplicity, we put the remnants of the nonperturbative effects beyond the deconfinement temperature by a multiplication factor of 1.4 to the leading-order Debye mass, to take into account the next-to-leading corrections [79] (the factor is also obtained by fitting with the lattice results for the color-singlet free energy [80]).

$$\begin{aligned}\text{Re}V_{(\text{iso})}(r, T) &= \int \frac{d^3 p}{(2\pi)^{3/2}} (e^{i\mathbf{p}\cdot\mathbf{r}} - 1) \\ &\quad \times \left(-\sqrt{(2/\pi)} \frac{\alpha}{p^2} - \frac{4\sigma}{\sqrt{2\pi} p^4} \right) \left(\frac{p^2}{(p^2 + m_D^2)} \right) \\ &\equiv \text{Re}V_{1(\text{iso})}(r, T) + \text{Re}V_{2(\text{iso})}(r, T),\end{aligned}\quad (36)$$

where $\text{Re}V_{1(\text{iso})}(r, T)$ and $\text{Re}V_{2(\text{iso})}(r, T)$ correspond to the medium modifications to the Coulomb and string term, respectively. After performing the momentum integration, the Coulomb term becomes

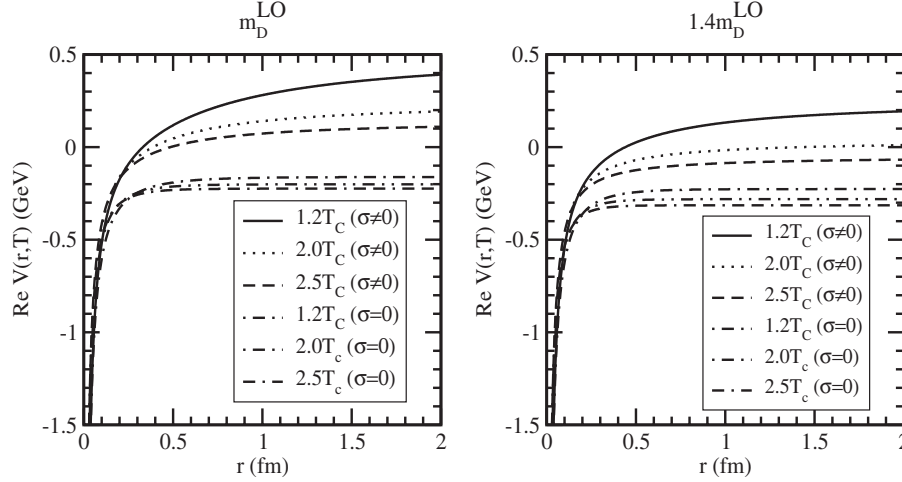


FIG. 1. Real part of the static potential with ($\sigma = 0$) and without a ($\sigma \neq 0$) nonperturbative term in the potential. The left (right) panel of the figure denotes the results obtained with the leading-order and lattice-fitted Debye masses, respectively.

$$\text{Re}V_{1(\text{iso})}(r, T) = -am_D \left(\frac{e^{-\hat{r}}}{\hat{r}} + 1 \right) \quad (37)$$

and the string term simplifies into

$$\text{Re}V_{2(\text{iso})}(r, T) = \frac{2\sigma}{m_D} \left(\frac{e^{-\hat{r}} - 1}{\hat{r}} + 1 \right). \quad (38)$$

The real part of the potential in the isotropic medium becomes (with $\hat{r} = rm_D$)

$$\text{Re}V_{(\text{iso})}(\hat{r}, T) = \left(\frac{2\sigma}{m_D} - am_D \right) \frac{e^{-\hat{r}}}{\hat{r}} - \frac{2\sigma}{m_D \hat{r}} + \frac{2\sigma}{m_D} - am_D, \quad (39)$$

which is found to have an additional long-range Coulomb term, in addition to the conventional Yukawa term. In the small-distance limit ($\hat{r} \ll 1$), the above potential reduces to the Cornell potential, i.e., the $Q\bar{Q}$ -pair does not see the medium. On the other hand, in the long-distance limit ($\hat{r} \gg 1$), the potential is simplified into, with the high temperature approximation (i.e., $\sigma/m_D(T)$ can be neglected),

$$\text{Re}V_{(\text{iso})}(r, T) \approx -\frac{2\sigma}{m_D^2 r} - am_D, \quad (40)$$

which, apart from a constant term, is a Coulomb-like potential by identifying $2\sigma/m_D^2$ with the square of the strong coupling (g^2). However, if we compare the asymptotic limit ($r \rightarrow \infty$) of our result (39) with the Digal *et al.*

$$F^{\text{Digal}}(\infty, T) = \frac{\Gamma(1/4)}{2^{3/2}\Gamma(3/4)} \frac{\sigma}{m_D(T)} - am_D(T)$$

$$F^{\text{Our}}(\infty, T) = \frac{2\sigma}{m_D(T)} - am_D(T),$$

the difference will be seen in the string term only and may be due to the treatment of the problem classically or quantum mechanically. If we compare them quantitatively (with the Debye mass $m_D = 1.4m_D^{\text{LO}}$), the difference becomes tiny.

To see the effect of the linear term on the potential, in addition to the Coulomb term, we have plotted the (real-part) potential (in Fig. 1) with ($\sigma \neq 0$) and without string term ($\sigma = 0$). We found that the inclusion of the linear term makes the potential attractive, compared to the potential with the Coulomb term only. Furthermore, to see the effects of the screening scale, we have also computed the potential with the Debye mass in the next-to-leading order ($1.4m_D^{\text{LO}}$), which is seen as less strong than the leading-order result. To see the effects of the medium on the potential at $T = 0$, we have evaluated the potential at different temperatures, viz., at $1.2T_c$, $2.0T_c$, and $2.5T_c$, where the potential is found to decrease with the temperature at large distances and becomes short range. Thus, the deconfinement is reflected clearly in the large-distance behavior of heavy quark potential at finite temperature, where the screening is operative. Thus, the in-medium behavior of heavy quark bound states is used to probe the state of matter in QCD thermodynamics.²

2. Imaginary part of the potential: Thermal width, Γ_{iso}

The imaginary part of the potential originates from the static limit of symmetric self energy. Cutting rules at finite temperature allows one to obtain the imaginary part by cutting open one of the hard thermal loops of the HTL propagator, which represents physically the inelastic scattering of the off-shell gluon off a thermal gluon

²The real part of the singlet potential indeed coincides with the leading-order result of the so-called singlet free energy [80] because it contains entropy contribution.

[10,17,32,63], i.e., $g + (Q\bar{Q}) \rightarrow g + Q + \bar{Q}$. The imaginary part of the potential plays an important role in weakening the bound state peak or transforming it to mere threshold enhancement. It leads to a finite width (Γ) for the resonance peak in the spectral function, which, in turn, determines the dissociation temperature. Dissociation is expected to occur while the (twice) binding energy decreases with the temperature and becomes equal to $\sim\Gamma$ [23,31].

To obtain the imaginary part of the potential in the isotropic medium, we write the temporal component of the symmetric propagator from (30) for $\xi = 0$, in the static limit, as

$$\text{Im}D_{F(\text{iso})}^{00}(0, p) = \frac{-2\pi T m_D^2}{p(p^2 + m_D^2)^2}. \quad (41)$$

However, the same (41) could also be obtained for partons with space-like momenta ($p_0^2 < p^2$) from the retarded (advanced) self energy (24) using the relation [17,59]

$$\ln \frac{p_0 + p \pm i\epsilon}{p_0 - p \pm i\epsilon} = \ln \left| \frac{p_0 + p}{p_0 - p} \right| \mp i\pi\theta(p^2 - p_0^2). \quad (42)$$

Thus, the imaginary part of the symmetric propagator (41) gives the imaginary part of the dielectric function in the isotropic medium:

$$\epsilon^{-1}(p) = -\pi T m_D^2 \frac{p^2}{p(p^2 + m_D^2)^2}. \quad (43)$$

One can then similarly find the imaginary part of the potential from the definition of the potential (1):

$$\begin{aligned} \text{Im}V_{(\text{iso})}(r, T) &= - \int \frac{d^3\mathbf{p}}{(2\pi)^{3/2}} (e^{i\mathbf{p}\cdot\mathbf{r}} - 1) \\ &\times \left(-\sqrt{\frac{2}{\pi}} \frac{\alpha}{p^2} - \frac{4\sigma}{\sqrt{2\pi}p^4} \right) p^2 \left[\frac{-\pi T m_D^2}{p(p^2 + m_D^2)^2} \right] \\ &\equiv \text{Im}V_{1(\text{iso})}(r, T) + \text{Im}V_{2(\text{iso})}(r, T), \end{aligned} \quad (44)$$

where $\text{Im}V_{1(\text{iso})}(r, T)$ and $\text{Im}V_{2(\text{iso})}(r, T)$ are the imaginary parts of the potential due to the medium modification to the short-distance and long-distance terms, respectively:

$$\begin{aligned} \text{Im}V_{1(\text{iso})}(r, T) &= -\frac{\alpha}{2\pi^2} \int d^3\mathbf{p} (e^{i\mathbf{p}\cdot\mathbf{r}} - 1) \left[\frac{\pi T m_D^2}{p(p^2 + m_D^2)^2} \right], \\ \text{Im}V_{2(\text{iso})}(r, T) &= -\frac{4\sigma}{(2\pi)^2} \int \frac{d^3\mathbf{p}}{(2\pi)^{3/2}} (e^{i\mathbf{p}\cdot\mathbf{r}} - 1) \frac{1}{p^2} \left[\frac{\pi T m_D^2}{p(p^2 + m_D^2)^2} \right]. \end{aligned} \quad (45)$$

After performing the integration, the contribution due to the short-distance term to the imaginary part becomes (with $z = p/m_D$)

$$\begin{aligned} \text{Im}V_{1(\text{iso})}(r, T) &= -2\alpha T \int_0^\infty \frac{dz}{(z^2 + 1)^2} \left(1 - \frac{\sin z\hat{r}}{z\hat{r}} \right) \\ &\equiv -\alpha T \phi_0(\hat{r}), \end{aligned} \quad (46)$$

and the contribution due to the string term becomes

$$\begin{aligned} \text{Im}V_{2(\text{iso})}(r, T) &= \frac{4\sigma T}{m_D^2} \int_0^\infty \frac{dz}{z(z^2 + 1)^2} \left(1 - \frac{\sin z\hat{r}}{z\hat{r}} \right) \\ &\equiv \frac{2\sigma T}{m_D^2} \psi_0(\hat{r}), \end{aligned} \quad (47)$$

where the functions, $\phi_0(\hat{r})$ and $\psi_0(\hat{r})$, at the leading order in \hat{r} are

$$\phi_0(\hat{r}) = -\alpha T \left(-\frac{\hat{r}^2}{9} (-4 + 3\gamma_E + 3 \log \hat{r}) \right) \quad (48)$$

$$\psi_0(\hat{r}) = \frac{\hat{r}^2}{6} + \left(\frac{-107 + 60\gamma_E + 60 \log(\hat{r})}{3600} \right) \hat{r}^4 + O(\hat{r}^5). \quad (49)$$

In the short-distance limit ($\hat{r} \ll 1$), both the contributions, at the leading logarithmic order, reduce to

$$\text{Im}V_{1(\text{iso})}(r, T) = -\alpha T \frac{\hat{r}^2}{3} \log \left(\frac{1}{\hat{r}} \right), \quad (50)$$

$$\text{Im}V_{2(\text{iso})}(r, T) = -\frac{2\sigma T}{m_D^2} \frac{\hat{r}^4}{60} \log \left(\frac{1}{\hat{r}} \right); \quad (51)$$

thus, the sum of the Coulomb and string term gives the imaginary part of the potential in the isotropic medium:

$$\text{Im}V_{(\text{iso})}(r, \xi, T) = -T \left(\frac{\alpha \hat{r}^2}{3} + \frac{\sigma \hat{r}^4}{30m_D^2} \right) \log \left(\frac{1}{\hat{r}} \right). \quad (52)$$

One thus immediately observes that for small distances the imaginary part vanishes and its magnitude is larger than the case where only the Coulombic term is considered [65] and thus enhances the width of the resonances in the thermal medium.

The imaginary part of the potential, in the small-distance limit, is a perturbation to the vacuum potential and thus provides an estimate for the width (Γ) for a resonance state and can be calculated, in a first-order perturbation, by folding with the unperturbed (1S) Coulomb wave function

$$\Gamma_{(\text{iso})} = \left(\frac{4T}{\alpha m_Q^2} + \frac{12\sigma T}{\alpha^2 m_Q^4} \right) m_D^2 \log \frac{\alpha m_Q}{2m_D}. \quad (53)$$

The main features of our results on the thermal width in Fig. 2 are the following: First, the width always increases with the temperature. Second, the inclusion of the

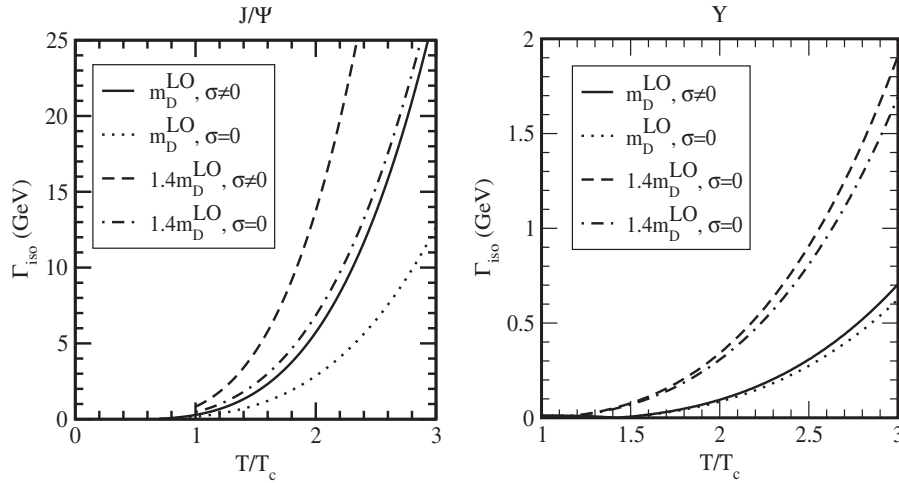


FIG. 2. Decay width of J/ψ (left) and Υ (right) states with and without nonperturbative (string) term in an isotropic medium with the Debye masses in leading-order and the lattice fitted result.

nonvanishing nonperturbative string term, in addition to the Coulomb term, makes the width larger than the earlier result with the perturbative Coulomb term [81] only and thus the damping of the exchanged gluon in the heat bath provides a larger contribution to the dissociation rate and consequently reduces the yield of dileptons in the peak. The effect of the nonperturbative term on the width is relatively more on the J/ψ than Υ state because the binding of the Υ (1S) state is more Coulombic than the J/ψ (1S) state. This may have far reaching implications on the dissociation in the medium. Third, the width is also affected by the screening scale we chose to regulate the potential, namely, the width with the higher screening scale ($1.4m_D^{\text{LO}}$) is more than the leading-order result because the width, Γ , increases with the increase of the Debye mass.

3. Real and imaginary binding energies: Dissociation temperatures

To understand the in-medium properties of the quarkonium states, one needs to solve the Schrödinger equation with both the real and imaginary parts of the finite temperature potential. As seen earlier, in the short-distance limit, the vacuum contribution dominates over the medium contribution, whereas in the long-distance limit the real part of the potential reduces to a Coulomb-like potential and thus yields the real part of the binding energy in the isotropic medium:

$$\text{Re}E_{\text{bin}}^{\text{iso}} \stackrel{\hat{r} \gg 1}{\approx} \left(\frac{m_Q \sigma^2}{m_D^4 n^2} + am_D \right); \quad n = 1, 2, \dots \quad (54)$$

However, in the intermediate-distance ($rm_D \approx 1$) scale, the interaction becomes complicated and the potential does not look simpler in contrast to the asymptotic limits; thus, the complex potential in general needs to be dealt with numerically to obtain the real and imaginary binding

energies. There are some numerical methods to solve the Schrödinger equation either in partial differential form (time-dependent) or eigenvalue form (time-independent) by the finite difference time domain method or matrix method, respectively. In the latter method, the stationary Schrödinger equation can be solved in a matrix form through a discrete basis, instead of the continuous real-space position basis spanned by the states $|\vec{x}\rangle$. Here, the confining potential V is subdivided into N discrete wells with potentials V_1, V_2, \dots, V_{N+2} such that for the i th boundary potential, $V = V_i$ for $x_{i-1} < x < x_i; i = 2, 3, \dots, (N+1)$. Therefore, for the existence of a bound state, there must be an exponentially decaying wave function in the region $x > x_{N+1}$ as $x \rightarrow \infty$ and has the form

$$\Psi_{N+2}(x) = P_E \exp[-\gamma_{N+2}(x - x_{N+1})] + Q_E \exp[\gamma_{N+2}(x - x_{N+1})], \quad (55)$$

where $P_E = \frac{1}{2}(A_{N+2} - B_{N+2})$, $Q_E = \frac{1}{2}(A_{N+2} + B_{N+2})$, and $\gamma_{N+2} = \sqrt{2\mu(V_{N+2} - E)}$. The eigenvalues can be obtained by identifying the zeros of Q_E .

The binding energies shown in Fig. 3 have the following features: First, when the nonperturbative term is included, the (real-part) binding of $Q\bar{Q}$ pairs gets stronger with respect to the case where only the Coulomb term is included. Second, there is a strong decreasing trend with the temperature because the screening becomes stronger with the increase of the temperature, so the real part of the potential becomes weaker compared to $T = 0$ and results in early dissolution of quarkonia in the medium. Third, the real part of the binding energy decreases with the increase of the screening scale ($1.4m_D^{\text{LO}}$). On the other hand, the imaginary part of the binding energy increases with the temperature. Thus, the study of both the binding energies is poised to provide a wealth of information about the dissociation pattern of quarkonium states in the thermal

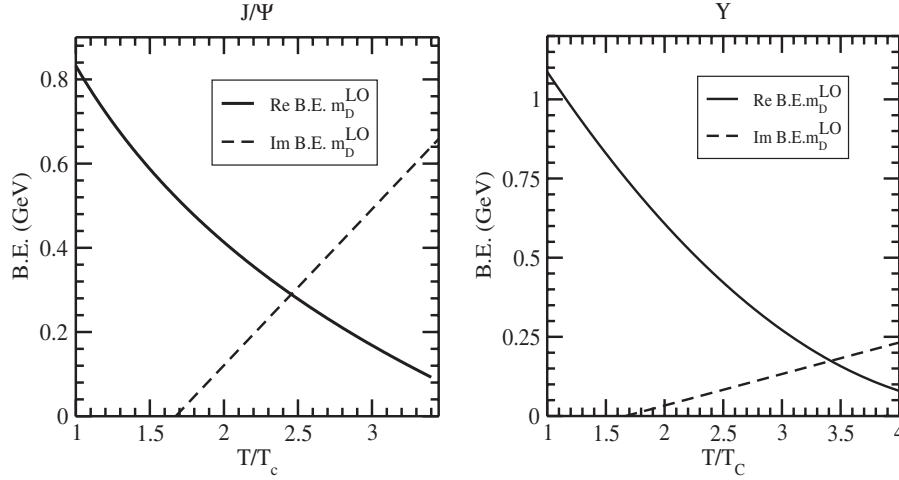


FIG. 3. Variation of the real and imaginary binding energies for the J/ψ and Υ states with the temperature (in units of critical temperature, T_c) in the left and right panel, respectively in an isotropic medium.

medium, which will be used to determine the dissociation temperatures.

We will now study the dissociation in the thermal medium to calculate the dissociation temperature (T_d) either from the intersection of the (real and imaginary) binding energies [42,61], or from the conservative criterion on the width of the resonance as $\Gamma \geq 2\text{Re B.E.}$ [23]. Although both definitions are physically equivalent, they are numerically different (Table I). For example, J/ψ is dissociated at $2.45 T_c$ obtained from the intersection of binding energies while the condition on width gives a much lower temperature ($1.40 T_c$). Correspondingly, Υ (1S) is dissociated at $3.40 T_c$ and $3.10 T_c$, respectively. Our results are found to be relatively higher compared to a similar calculation [42,61], which may be due to the absence of a three-dimensional medium modification of the linear term in their calculation.

Finally, we explore the sensitivity of the screening scale on the dissociation mechanism where the dissociation temperatures computed with the next-to-leading order ($1.4m_D^{\text{LO}}$) Debye mass are found to be smaller than the leading-order result (Table II). For example, J/ψ s and Υ s are now dissociated at $1.33 T_c$ and $1.91 T_c$, respectively.

C. Potential in the anisotropic medium

The space-time evolution of QGP relies on the viscous hydrodynamical treatment where the system assumes a

local thermal equilibrium, i.e., close to isotropic in momentum space, which may not be true at the very early time in the collision of two nuclei, due to large momentum-space anisotropies [74,82,83]. The degree of anisotropy increases as the shear viscosity increases and thus one must address it while calculating the heavy quark potential in the presence of momentum-space anisotropies. The real part of the heavy quark potential was first considered in [57] and then the imaginary part was obtained theoretically [59,60,84] as well as phenomenologically [42,58,61]. The main effect of the anisotropy is to reduce Debye screening, which, in turn has the effect that heavy quarkonium states can survive up to higher temperatures. However, the aforesaid works in the anisotropic medium are limited to the medium modification of the perturbative part only, and the nonperturbative string term was assumed to be zero. However, the string tension is nonvanishing even at temperatures much beyond the deconfinement point [49–51], so one should study its effect on the heavy quark potential in the anisotropic medium too.

1. Real part of the potential

Like in the isotropic medium, we obtain the real part of the potential in the weakly anisotropic medium [62] from the anisotropic corrections to the (temporal component) real part of the retarded propagator (29):

TABLE I. Dissociation temperatures of J/ψ and Υ states for different anisotropies with the Debye mass in the leading order.

Method	State	$\xi = 0.0$	$\xi = 0.3$	$\xi = 0.6$
Re B.E. = Im B.E.	J/ψ	2.45	2.46	2.47
	Υ	3.40	3.45	3.46
$\Gamma = 2\text{B.E.}$	J/ψ	1.40	1.46	1.54
	Υ	3.10	3.17	3.26

TABLE II. The same as Table I, but having the Debye mass ($m_D = 1.4m_D^{\text{LO}}$).

Method	State	$\xi = 0.0$	$\xi = 0.3$	$\xi = 0.6$
Re B.E. = Im B.E.	J/ψ	1.33	1.34	1.35
	Υ	1.91	1.93	1.94
$\Gamma = 2\text{B.E.}$	J/ψ	1.02	1.06	1.12
	Υ	1.88	1.92	2.02

$$\begin{aligned} \text{Re}V_{(\text{aniso})}(\mathbf{r}, \xi, T) &= \int \frac{d^3\mathbf{p}}{(2\pi)^{3/2}} (e^{i\mathbf{p}\cdot\mathbf{r}} - 1) \left(-\sqrt{(2/\pi)} \frac{\alpha}{p^2} - \frac{4\sigma}{\sqrt{2\pi}p^4} \right) \times p^2 \left[\frac{1}{(p^2 + m_D^2)} - \frac{\xi m_D^2}{6(p^2 + m_D^2)^2} (3 \cos(2\theta_p) - 1) \right] \\ &\equiv \text{Re}V_{1(\text{aniso})}(\mathbf{r}, \xi, T) + \text{Re}V_{2(\text{aniso})}(\mathbf{r}, \xi, T), \end{aligned} \quad (56)$$

where $\text{Re}V_{1(\text{aniso})}(\mathbf{r}, \xi, T)$ and $\text{Re}V_{2(\text{aniso})}(\mathbf{r}, \xi, T)$ are the medium modifications corresponding to the Coulomb and string term, respectively, and are given by

$$\text{Re}V_{1(\text{aniso})}(\mathbf{r}, \xi, T) = -\frac{\alpha}{2\pi^2} \int d^3\mathbf{p} (e^{i\mathbf{p}\cdot\mathbf{r}} - 1) \left[\frac{1}{(p^2 + m_D^2)} - \frac{\xi m_D^2}{6(p^2 + m_D^2)^2} (3 \cos 2\theta_p - 1) \right] \quad (57)$$

$$\text{Re}V_{2(\text{aniso})}(\mathbf{r}, \xi, T) = -\frac{4\sigma}{2\pi^2} \int d^3\mathbf{p} (e^{i\mathbf{p}\cdot\mathbf{r}} - 1) \frac{1}{p^2} \left[\frac{1}{(p^2 + m_D^2)} - \frac{\xi m_D^2}{6(p^2 + m_D^2)^2} (3 \cos 2\theta_p - 1) \right]. \quad (58)$$

To perform the momentum integration, we use the transformation $\cos \theta_p = \cos \theta_r \cos \theta_{pr} + \sin \theta_r \sin \theta_{pr} \cos \phi_{pr}$, where θ_p and θ_r are the angles between \mathbf{p} and \mathbf{n} , \mathbf{r} , and \mathbf{n} , respectively, and θ_{pr} , ϕ_{pr} are the angular variables between the vectors \mathbf{p} and \mathbf{r} . So, after the integration, the Coulombic contribution to the potential becomes

$$\text{Re}V_{1(\text{aniso})}(\mathbf{r}, \xi, T) = -am_D \left[\frac{e^{-\hat{r}}}{\hat{r}} + 1 + \xi \left[\frac{(e^{-\hat{r}} - 1)}{6} + \left[e^{-\hat{r}} \left(\frac{1}{6} + \frac{1}{2\hat{r}} + \frac{1}{\hat{r}^2} \right) + \frac{(e^{-\hat{r}} - 1)}{\hat{r}^3} \right] \times (1 - 3\cos^2\theta_r) \right] \right], \quad (59)$$

and the string contribution is

$$\begin{aligned} \text{Re}V_{2(\text{aniso})}(\mathbf{r}, \xi, T) &= \frac{2\sigma}{m_D} \left[\frac{(e^{-\hat{r}} - 1)}{\hat{r}} + 1 + 2\xi \left[\left(\frac{(e^{-\hat{r}} - 1)}{6\hat{r}} + \frac{e^{-\hat{r}}}{12} + \frac{1}{6} \right) \right. \right. \\ &\quad \left. \left. + \left(e^{-\hat{r}} \left(\frac{1}{\hat{r}^2} + \frac{5}{12\hat{r}} + \frac{1}{12} \right) + \frac{1}{12\hat{r}} + \frac{(e^{-\hat{r}} - 1)}{\hat{r}^3} \right) (1 - 3\cos^2\theta_r) \right] \right]. \end{aligned} \quad (60)$$

Thus, the real part of the potential in the anisotropic medium becomes

$$\begin{aligned} \text{Re}V_{\text{aniso}}(r, \theta_r, T) &= \left(\frac{2\sigma}{m_D} - am_D \right) \frac{e^{-\hat{r}}}{\hat{r}} - \frac{2\sigma}{m_D \hat{r}} + \frac{2\sigma}{m_D} - am_D + \xi \left(\frac{2\sigma}{m_D} \frac{e^{-\hat{r}}}{\hat{r}} \left[\frac{e^{\hat{r}} - 1}{\hat{r}^2} - \frac{5e^{\hat{r}}}{12} + \frac{\hat{r}e^{\hat{r}}}{3} - \frac{1}{\hat{r}} + \frac{\hat{r}}{12} - \frac{1}{12} \right] \right. \\ &\quad - \frac{am_D}{2} \frac{e^{-\hat{r}}}{\hat{r}} \left[\frac{e^{\hat{r}} - 1}{\hat{r}^2} - \frac{1}{\hat{r}} - \frac{\hat{r}e^{\hat{r}}}{3} + \frac{\hat{r}}{6} - \frac{1}{2} \right] + \left(\frac{2\sigma}{m_D} \frac{e^{-\hat{r}}}{\hat{r}} \left[3 \frac{e^{\hat{r}} - 1}{\hat{r}^2} - \frac{e^{\hat{r}}}{4} - \frac{3}{\hat{r}} - \frac{\hat{r}}{4} - \frac{5}{4} \right] \right. \\ &\quad \left. \left. - \frac{am_D}{2} \frac{e^{-\hat{r}}}{\hat{r}} \left[3 \frac{e^{\hat{r}} - 1}{\hat{r}^2} - \frac{3}{\hat{r}} - \frac{\hat{r}}{2} - \frac{3}{2} \right] \right) \cos 2\theta_r \right) \\ &= \text{Re}V_{\text{iso}}(r, T) + V_{\text{tensor}}(r, \theta_r, T). \end{aligned} \quad (61)$$

Thus, the anisotropy in the momentum space introduces an angular (θ_r) dependence, in addition to the interparticle separation (r), to the real part of the potential, in contrast to the r -dependence only in an isotropic medium. The real potential becomes stronger with the increase of anisotropy (shown in Fig. 4) because the (anisotropic) Debye mass $m_D(\xi, T)$ (or, equivalently, the angular-dependent Debye mass $m_D(\theta_r, T)$) in an anisotropic medium is always smaller than in an isotropic medium. As a result, the screening of the Coulomb and string contribution is less accentuated, compared to the isotropic medium. In particular, the potential for quark pairs aligned in the direction of anisotropy is stronger than in the pairs aligned in the transverse direction.

2. Imaginary part of the potential: Thermal width, Γ_{aniso}

Recently, the imaginary part with a momentum-space anisotropy and its effects on the thermal widths of the resonance states have been studied [61,65,81,85], with the medium modification to the perturbative (Coulomb) term only. The imaginary part of the potential arises due to the singlet-to-octet transitions induced by the dipole vertex as well as due to the Landau damping in the plasma, i.e., scattering of the gluons with space-like momentum off the thermal excitations in the medium. We follow their work by including the medium corrections to both perturbative (Coulombic) and nonperturbative (string) terms in a weakly anisotropic medium. Like in the isotropic medium, we can

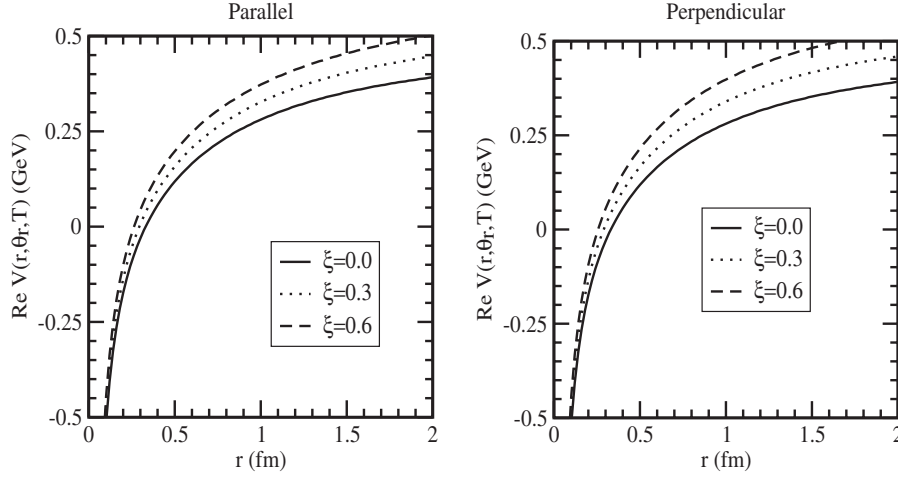


FIG. 4. Real part of the potential for both the parallel (left) and perpendicular (right) alignments with the Debye mass in the leading order.

obtain the imaginary part of the potential by the leading anisotropic correction to the imaginary part of the (temporal component) symmetric propagator as

$$\begin{aligned} \text{Im}V_{\text{(aniso)}}(\mathbf{r}, \xi, T) &= - \int \frac{d^3\mathbf{p}}{(2\pi)^{3/2}} (e^{i\mathbf{p}\cdot\mathbf{r}} - 1) \left(-\sqrt{\frac{2}{\pi}} \frac{\alpha}{p^2} - \frac{4\sigma}{\sqrt{2\pi}p^4} \right) \\ &\times p^2 \left[\frac{-\pi T m_D^2}{p(p^2 + m_D^2)^2} + \xi \left[\frac{3\pi T m_D^2}{2p(p^2 + m_D^2)^2} \sin^2\theta_p \right. \right. \\ &\left. \left. - \frac{4\pi T m_D^4}{p(p^2 + m_D^2)^3} \left(\sin^2\theta_p - \frac{1}{3} \right) \right] \right] \\ &\equiv \text{Im}V_{1\text{(aniso)}}(\mathbf{r}, \xi, T) + \text{Im}V_{2\text{(aniso)}}(\mathbf{r}, \xi, T), \end{aligned} \quad (62)$$

where $\text{Im}V_{1\text{(aniso)}}(\mathbf{r}, \xi, T)$ and $\text{Im}V_{2\text{(aniso)}}(\mathbf{r}, \xi, T)$ are the imaginary contributions corresponding to the Coulombic and linear terms in the anisotropic medium, respectively:

$$\begin{aligned} \text{Im}V_{1\text{(aniso)}}(\mathbf{r}, \xi, T) &= \frac{\alpha}{2\pi^2} \int d^3\mathbf{p} (e^{i\mathbf{p}\cdot\mathbf{r}} - 1) \left[\frac{-\pi T m_D^2}{p(p^2 + m_D^2)^2} \right. \\ &+ \xi \left[\frac{3\pi T m_D^2}{4p(p^2 + m_D^2)^2} \sin^2\theta_p \right. \\ &\left. \left. - \frac{2\pi T m_D^4}{p(p^2 + m_D^2)^3} \left(\sin^2\theta_p - \frac{1}{3} \right) \right] \right], \end{aligned} \quad (63)$$

$$\begin{aligned} \text{Im}V_{2\text{(aniso)}}(\mathbf{r}, \xi, T) &= \frac{4\sigma}{(2\pi)^2} \int \frac{d^3\mathbf{p}}{(2\pi)^{3/2}} (e^{i\mathbf{p}\cdot\mathbf{r}} - 1) \frac{1}{p^2} \left[\frac{-\pi T m_D^2}{p(p^2 + m_D^2)^2} \right. \\ &+ \xi \left[\frac{3\pi T m_D^2}{4p(p^2 + m_D^2)^2} \sin^2\theta_p \right. \\ &\left. \left. - \frac{2\pi T m_D^4}{p(p^2 + m_D^2)^3} \left(\sin^2\theta_p - \frac{1}{3} \right) \right] \right]. \end{aligned} \quad (64)$$

Since the isotropic contribution is already calculated in Sec. IIB2, so the anisotropic contribution to the perturbative term in the leading order is given by [65]

$$\text{Im}V_{1\text{(aniso)}}(\mathbf{r}, \xi, T) \equiv \alpha T \xi [\phi_1(\hat{r}, \theta_r) + \phi_2(\hat{r}, \theta_r)], \quad (65)$$

where the functions $\phi_1(\hat{r}, \theta_r)$ and $\phi_2(\hat{r}, \theta_r)$ are

$$\begin{aligned} \phi_1(\hat{r}, \theta_r) &= \frac{\hat{r}^2}{600} [123 - 90\gamma_E - 90 \log \hat{r} \\ &+ \cos(2\theta_r)(-31 + 30\gamma_E + 30 \log \hat{r})], \\ \phi_2(\hat{r}, \theta_r) &= \frac{\hat{r}^2}{90} (-4 + 3 \cos(2\theta_r)). \end{aligned} \quad (66)$$

Similarly, the imaginary contribution due to the nonperturbative (linear) term can also be separated into the isotropic and anisotropic terms, where the isotropic part is already calculated in Sec. IIB2 and hence the anisotropic part is now calculated:

$$\text{Im}V_{2\text{(aniso)}}(r, \xi, T) = -\xi \frac{2\sigma T}{m_D^2} [\psi_1(\hat{r}, \theta_r) + \psi_2(\hat{r}, \theta_r)]. \quad (67)$$

The function, $\psi_1(\hat{r}, \theta_r)$, is given by

$$\begin{aligned} \psi_1(\hat{r}, \theta_r) &= \int \frac{dz}{z(z^2 + 1)^2} \left[1 - \frac{3}{2} \left(\sin^2\theta_r \frac{\sin z\hat{r}}{z\hat{r}} \right. \right. \\ &\left. \left. + (1 - 3\cos^2\theta_r)G(\hat{r}, z) \right) \right], \end{aligned} \quad (68)$$

where $G(\hat{r}, z)$ is given by

$$G(\hat{r}, z) = \frac{z\hat{r} \cos(z\hat{r}) - \sin(z\hat{r})}{(z\hat{r})^3}. \quad (69)$$

Substituting $G(\hat{r}, z)$ into $\psi_1(\hat{r}, \theta_r)$ and decomposing into θ_r -dependent and -independent terms, the function, $\psi_1(\hat{r}, \theta_r)$, can be rewritten as

$$\begin{aligned} \psi_1(\hat{r}, \theta_r) &= \int \frac{dz}{z(z^2+1)^2} \left[1 - \frac{3}{2} \left(\frac{\sin(z\hat{r})}{z\hat{r}} + \frac{\cos(z\hat{r})}{(z\hat{r})^2} - \frac{\sin(z\hat{r})}{(z\hat{r})^3} \right) \right. \\ &\quad \left. + \frac{3}{2} \left(\frac{\sin(z\hat{r})}{z\hat{r}} + 3 \frac{\cos(z\hat{r})}{(z\hat{r})^2} - 3 \frac{\sin(z\hat{r})}{(z\hat{r})^3} \right) \cos^2 \theta_r \right] \\ &\equiv \psi_1^{(1)}(\hat{r}) + \psi_1^{(2)}(\hat{r}, \theta_r), \end{aligned} \quad (70)$$

where the functions $\psi_1^{(1)}(\hat{r})$ and $\psi_1^{(2)}(\hat{r}, \theta_r)$ are given by

$$\begin{aligned} \psi_1^{(1)}(\hat{r}) &= \int \frac{dz}{z(z^2+1)^2} \left[1 - \frac{3}{2} \left(\frac{\sin(z\hat{r})}{z\hat{r}} + \frac{\cos(z\hat{r})}{(z\hat{r})^2} - \frac{\sin(z\hat{r})}{(z\hat{r})^3} \right) \right] \\ &= \hat{r}^4 \int \frac{dx}{x(x^2+\hat{r}^2)^2} \left[1 - \frac{3}{2} \left(\frac{\sin(x)}{x} + \frac{\cos(x)}{x^2} - \frac{\sin(x)}{x^3} \right) \right] \\ &= \frac{\hat{r}^2}{10} + \frac{(-739+420\gamma_E+420\log(\hat{r}))\hat{r}^4}{39200} + O(\hat{r}^5), \end{aligned} \quad (71)$$

$$\begin{aligned} \psi_1^{(2)}(\hat{r}, \theta_r) &= \frac{3}{2} \int \frac{dz}{z(z^2+1)^2} \left[\left(\frac{\sin(z\hat{r})}{z\hat{r}} + 3 \frac{\cos(z\hat{r})}{(z\hat{r})^2} - 3 \frac{\sin(z\hat{r})}{(z\hat{r})^3} \right) \cos^2 \theta_r \right] \\ &= \frac{3}{2} \hat{r}^4 \int \frac{dx}{x(x^2+\hat{r}^2)^2} \left[\left(\frac{\sin(x)}{x} + \frac{3 \cos(x)}{x^2} - \frac{3 \sin(x)}{x^3} \right) \cos^2 \theta_r \right] \\ &= \left(-\frac{\hat{r}^2}{20} + \frac{(176-105\gamma_E-105\log(\hat{r}))\hat{r}^4}{14700} + O(\hat{r}^5) \right) \cos^2 \theta_r. \end{aligned} \quad (72)$$

The remaining function in the imaginary part of the potential associated with the linear term (67) can similarly be separated into θ_r -dependent and -independent terms:

$$\begin{aligned} \psi_2(\hat{r}, \theta_r) &= -\frac{4}{3} \int \frac{dz}{z(z^2+1)^3} \left[1 - 3 \left[\left(\frac{2}{3} - \cos^2 \theta_r \right) \frac{\sin z\hat{r}}{z\hat{r}} + (1 - 3\cos^2 \theta_r) G(\hat{r}, z) \right] \right] \\ &= -\frac{4}{3} \int \frac{dz}{z(z^2+1)^3} \left[\left(1 - \frac{2 \sin z\hat{r}}{z\hat{r}} - \frac{3 \cos(z\hat{r})}{(z\hat{r})^2} + \frac{3 \sin(z\hat{r})}{(z\hat{r})^3} \right) + 3 \left(\frac{\sin z\hat{r}}{z\hat{r}} + \frac{3 \cos(z\hat{r})}{(z\hat{r})^2} - \frac{3 \sin(z\hat{r})}{(z\hat{r})^3} \right) \cos^2 \theta_r \right] \\ &\equiv \psi_2^{(1)}(\hat{r}) + \psi_2^{(2)}(\hat{r}, \theta_r), \end{aligned} \quad (73)$$

where the functions $\psi_2^{(1)}(\hat{r})$ and $\psi_2^{(2)}(\hat{r}, \theta_r)$ are given by

$$\begin{aligned} \psi_2^{(1)}(\hat{r}) &= -\frac{4}{3} \int \frac{dz}{z(z^2+1)^3} \left(1 - \frac{2 \sin z\hat{r}}{z\hat{r}} - \frac{3 \cos(z\hat{r})}{(z\hat{r})^2} + \frac{3 \sin(z\hat{r})}{(z\hat{r})^3} \right) \\ &= -\frac{4}{3} \left[\frac{7\hat{r}^2}{120} - \frac{11\hat{r}^4}{3360} + O(\hat{r}^5) \right], \end{aligned} \quad (74)$$

and

$$\begin{aligned} \psi_2^{(2)}(\hat{r}, \theta_r) &= -4 \int \frac{dz}{z(z^2+1)^3} \left(\frac{\sin z\hat{r}}{z\hat{r}} + \frac{3 \cos(z\hat{r})}{(z\hat{r})^2} - \frac{3 \sin(z\hat{r})}{(z\hat{r})^3} \right) \cos^2 \theta_r \\ &= -4 \left[-\frac{\hat{r}^2}{60} + \frac{\hat{r}^4}{840} + O(\hat{r}^5) \right] \cos^2 \theta_r. \end{aligned} \quad (75)$$

So the functions $\psi_1(\hat{r}, \theta_r)$ and $\psi_2(\hat{r}, \theta_r)$ are finally given by

$$\begin{aligned} \psi_1(\hat{r}, \theta_r) &= \frac{\hat{r}^2}{10} + \frac{(-739+420\gamma_E+420\log(\hat{r}))\hat{r}^4}{39200} \\ &\quad + \left(-\frac{\hat{r}^2}{20} + \frac{(176-105\gamma_E-105\log(\hat{r}))\hat{r}^4}{14700} \right) \cos^2 \theta_r, \end{aligned} \quad (76)$$

$$\begin{aligned} \psi_2(\hat{r}, \theta_r) &= -\frac{4}{3} \left[\frac{7\hat{r}^2}{120} - \frac{11\hat{r}^4}{3360} + O(\hat{r}^5) \right] \\ &\quad - 4 \left[-\frac{\hat{r}^2}{60} + \frac{\hat{r}^4}{840} + O(\hat{r}^5) \right] \cos^2 \theta_r, \end{aligned} \quad (77)$$

respectively, and γ_E is the Euler-Gamma constant. Finally, the short and long-distance contributions, in the leading logarithmic order,

$$\text{Im}V_{1(\text{aniso})}(r, \theta_r, T) = -\alpha T \hat{r}^2 \log\left(\frac{1}{\hat{r}}\right) \left(\frac{1}{3} - \xi \frac{3 - \cos 2\theta_r}{20}\right), \quad (78)$$

$$\text{Im}V_{2(\text{aniso})}(r, \theta_r, T) = -\frac{2\sigma T \hat{r}^4}{m_D^2 20} \log\left(\frac{1}{\hat{r}}\right) \left(\frac{1}{3} - \xi \frac{2 - \cos 2\theta_r}{14}\right), \quad (79)$$

gives the imaginary part of the potential in the anisotropic medium

$$\begin{aligned} \text{Im}V_{(\text{aniso})}(r, \theta_r, T) &= -T \left(\frac{\alpha \hat{r}^2}{3} + \frac{\sigma \hat{r}^4}{30m_D^2} \right) \log\left(\frac{1}{\hat{r}}\right) + \xi T \left[\left(\frac{\alpha \hat{r}^2}{5} + \frac{3\sigma \hat{r}^4}{140m_D^2} \right) \right. \\ &\quad \left. - \cos^2\theta_r \left(\frac{\alpha \hat{r}^2}{10} + \frac{\sigma \hat{r}^4}{70m_D^2} \right) \right] \log\left(\frac{1}{\hat{r}}\right), \quad (80) \end{aligned}$$

which is found to be smaller than the isotropic medium and decreases with the increase of anisotropy (shown in Fig. 5).

Like in the isotropic medium, in the weakly anisotropic medium, too, the imaginary part is found to be a perturbation and thus provides an estimate for the (thermal) width for a particular resonance state:

$$\begin{aligned} \Gamma_{(\text{aniso})} &= \int d^3\mathbf{r} |\Psi(r)|^2 \left[\alpha T \hat{r}^2 \log\left(\frac{1}{\hat{r}}\right) \left(\frac{1}{3} - \xi \frac{3 - \cos 2\theta_r}{20}\right) \right. \\ &\quad \left. + \frac{2\sigma T}{m_D^2} \hat{r}^4 \log\left(\frac{1}{\hat{r}}\right) \frac{1}{20} \left(\frac{1}{3} - \xi \frac{2 - \cos 2\theta_r}{14}\right) \right] \\ &= T \left(\frac{4}{\alpha m_Q^2} + \frac{12\sigma}{\alpha^2 m_Q^4} \right) \left(1 - \frac{\xi}{2}\right) m_D^2 \log \frac{\alpha m_Q}{2m_D}, \quad (81) \end{aligned}$$

which shows that the width in the anisotropic medium becomes smaller than in the isotropic medium and gets narrower with the increase of anisotropy (shown in Fig. 6). This is due to the fact that Γ is approximately proportional

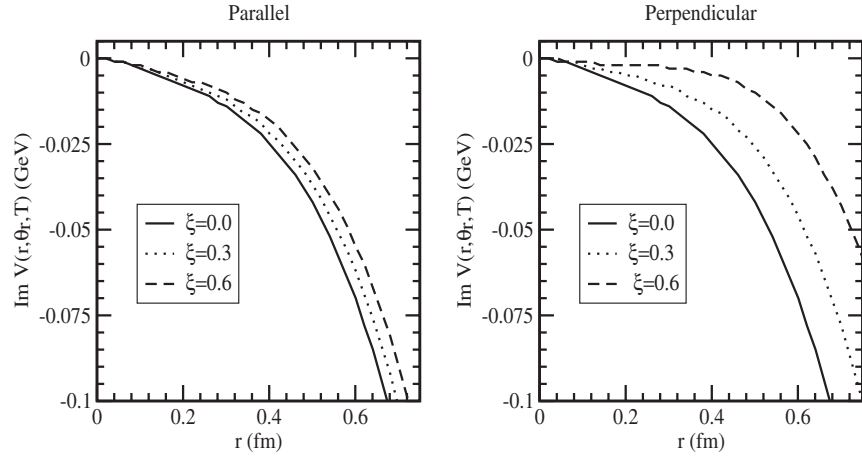


FIG. 5. Imaginary part of the potential for parallel (left) and perpendicular (right) alignments in an anisotropic medium.

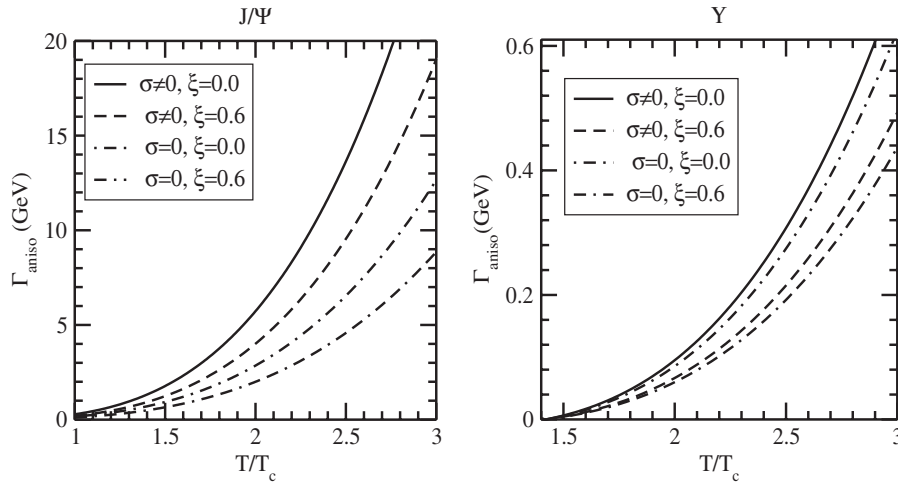


FIG. 6. Thermal width for the J/ψ and Υ states in the anisotropic medium.

to the (square) Debye mass and the Debye mass decreases in the anisotropic medium because the effective local parton density around a test (heavy) quark is smaller compared to the isotropic medium.

3. Real and imaginary binding energies: Dissociation temperatures

The real part of the potential thus obtained in the anisotropic medium (61), in contrast to its counterpart (the spherically symmetric potential), in the isotropic medium Eq. (39) is nonspherical and so one cannot simply obtain the energy eigenvalues by solving the radial part of the Schrödinger equation alone because the radial part is no longer sufficient due to the angular dependence in the potential. Another way to understand is that because of the anisotropic screening scale, the wave functions are no longer radially symmetric for $\xi \neq 0$. So one has to solve the potential in three dimensions but, in the small ξ -limit, the nonsymmetric component $V_{\text{tensor}}(r, \theta_r, T)$ is much smaller than the symmetric (isotropic) component $\text{Re}V_{\text{iso}}(r, T)$ and thus can be treated as a perturbation. Therefore, the corrected energy eigenvalues come from the solution of the Schrödinger equation of the isotropic component plus the first-order perturbation due to the anisotropic component $V_{\text{tensor}}(r, \theta_r, T)$.

In the short-distance limit, the vacuum contribution dominates over the medium contribution even for the weakly anisotropic medium and, in the long-distance limit, the real part of the potential in high temperature approximation results in a Coulomb plus a subleading anisotropic contribution:

$$\text{Re}V_{\text{(aniso)}}(r, \theta_r, T) \stackrel{\hat{r} \gg 1}{\cong} -\frac{2\sigma}{m_D^2 r} - \alpha m_D - \frac{5\xi}{12} \frac{2\sigma}{m_D^2 r} \times \left(1 + \frac{3}{5} \cos 2\theta_r\right) \quad (82)$$

$$\equiv \text{Re}V_{\text{iso}}(\hat{r} \gg 1, T) + V_{\text{tensor}}(\hat{r} \gg 1, \theta_r, T), \quad (83)$$

where the anisotropic contribution ($V_{\text{tensor}}(\hat{r} \gg 1, \theta_r, T)$) is smaller than the isotropic one ($\text{Re}V_{\text{iso}}(\hat{r} \gg 1, T)$), so the anisotropic part can be treated as a perturbation. Therefore, the real part of the binding energy may be obtained from the radial part of the Schrödinger equation (of the isotropic component) plus the first-order perturbation due to the anisotropic component as

$$\text{Re}E_{\text{bin}}^{\text{aniso}} = \left(\frac{m_Q \sigma^2}{m_D^4 n^2} + \alpha m_D\right) + \frac{2\xi}{3} \frac{m_Q \sigma^2}{m_D^4 n^2}, \quad (84)$$

where the first term is the solution of the (radial part) of the Schrödinger equation with the isotropic part ($\text{Re}V_{\text{iso}}(\hat{r} \gg 1, T)$) and the second term being due to the anisotropic perturbation of the tensorial component ($V_{\text{tensor}}(\hat{r} \gg 1, \theta_r, T)$) calculated from the first-order perturbation theory.

The real and imaginary parts of the binding energies for the J/ψ and Υ states are computed numerically in Fig. 7 for different values of anisotropies, with the following observations: The inclusion of the nonperturbative string term makes the quarkonium states more bound in the anisotropic medium, too. Second, the binding of $Q\bar{Q}$ pairs becomes stronger with respect to their isotropic counterpart and increases with the increase of anisotropy because the (real part) potential becomes deeper due to the weaker screening. Last but not the least, as the screening scale increases, the binding gets weakened even in the anisotropic medium. In contrast to the real part of the binding energy, the imaginary part of the binding energy increases with the temperature but increases with the anisotropy. With these observations, we have now computed the dissociation temperatures at different anisotropies (Table I), where J/ψ is dissociated at $2.46T_c$ and $2.49T_c$ for $\xi = 0.3$ and 0.6 , respectively (obtained from the intersection of binding energies), whereas Υ s are dissociated at $3.45T_c$ and $3.46T_c$, respectively. Thus, the presence of anisotropy enhances the dissociation point to

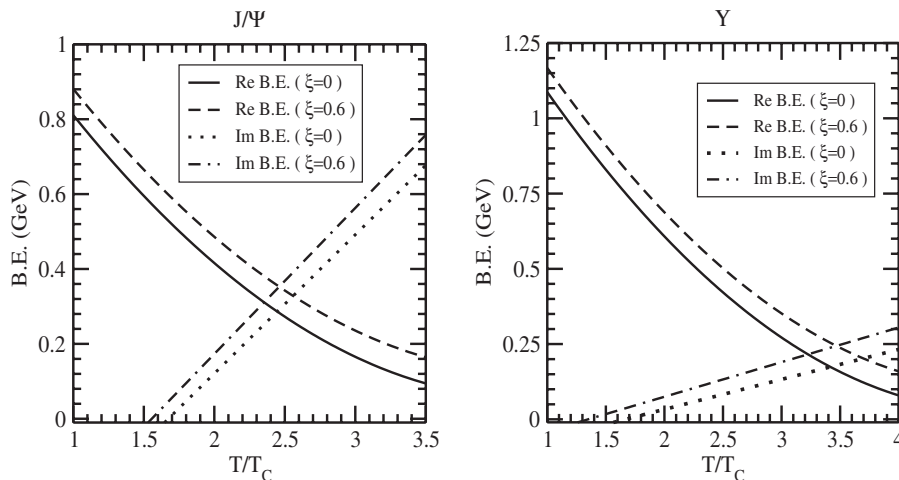


FIG. 7. Variation of the real and imaginary part of the binding energies for J/ψ and Υ states for different anisotropies.

the resonances. Like in the isotropic medium, we also computed the dissociation temperatures from the criterion on the thermal width and found that the temperatures become smaller. For example, J/ψ is now dissociated at $1.46T_c$ and $1.54T_c$ and Υ is dissociated at $3.17T_c$ and $3.26T_c$ for the same anisotropies.

III. CONCLUSION

We have investigated the properties of charmonium and bottomonium states through the in-medium modifications to both perturbative and nonperturbative terms of the Cornell potential, not its perturbative term alone, as is usually done in the literature. For this purpose, we have obtained both the real and imaginary parts of the potential within the framework of real-time formalism, in both the isotropic and anisotropic mediums. In the isotropic medium, the inclusion of the linear/string term, in addition to the Coulomb term, makes the real part of the potential more attractive. So, as a consequence, the quarkonium states become more bound compared to the medium modification to the Coulomb term alone. Moreover, the string term affects the imaginary part, too, where its magnitude is increased by the string contribution. As a result, the (thermal) width of the states are broadened due to the presence of the string term and makes the competition between the screening and the broadening due to damping interesting and plays an important role in the dissociation mechanism. With these cumulative observations, we studied the dissociation in a medium where a resonance is said to be dissolved in a medium [32,59] either when its (real) binding energy decreases with temperature and becomes equal to its width or the real and imaginary binding energy becomes equal. We have found that the quarkonium states are dissociated at a higher temperature compared to the medium consideration of the Coulomb term only.

We then extended our exploration of quarkonium to a medium that exhibits a local anisotropy in the momentum space. This may arise due to the rapid expansion in the beam direction compared to its transverse direction, at the early stage of the evolution in ultrarelativistic heavy-ion collisions. For that, we have first revisited the anisotropic corrections to the retarded, advanced, and symmetric propagators through their self energies in the hard-loop resummation technique and we apply these results to calculate the medium corrections to the perturbative and nonperturbative terms of the Cornell potential. We are, however, restricted to a medium

closer to equilibrium/isotropic because, although the system was initially anisotropic, by the time quarkonium resonances are formed in plasma ($t_F = \gamma\tau_F$, τ_F is the formation time in the rest frame of quarkonium), the plasma becomes almost isotropic.

The effect of the nonvanishing nonperturbative term on the quarkonium properties, as seen earlier, remains the same even in the presence of momentum anisotropy. However, the anisotropy behaves as an additional handle to decipher the properties of quarkonium states, namely, in the anisotropic medium, the binding of $Q\bar{Q}$ pairs gets stronger with respect to their isotropic counterpart because both the real and imaginary parts of the complex potential become deeper with the increase of anisotropy. This is due to the fact that the (effective) Debye mass in the anisotropic medium is always smaller than in the isotropic medium. As a result, the screening of the Coulomb and string contributions is less accentuated and thus quarkonium states are bound more strongly than in the isotropic medium. The overall observation is that the dissociation temperature increases with the increase of anisotropy. For example, J/ψ is dissociated at $2.45T_c$, $2.46T_c$, and $2.49T_c$ for the anisotropies $\xi = 0, 0.3$, and 0.6 , respectively. Similarly, Υ is dissociated at $3.40T_c$, $3.45T_c$, and $3.46T_c$ for $\xi = 0, 0.3$, and 0.6 , respectively.

Our results on the dissociation temperatures are found to be relatively higher compared to a similar calculation [42,61], which may be due to the absence of the three-dimensional medium modification of the linear term in their calculation. In fact, the one-dimensional Fourier transform of the Cornell potential yields the similar form used in the lattice QCD in which a one-dimensional color flux tube structure was assumed [52]. However, at finite temperature that may not be the case since the flux tube structure may expand in more dimensions [53]. Therefore, it would be better to consider the three-dimensional form of the medium modified Cornell potential, which has been done exactly in the present work.

In brief, the properties of quarkonium states are affected by the inclusion of the nonperturbative (string) term in the potential, in addition to the anisotropic medium effects, which need more careful treatment in future due to their nonperturbative character.

ACKNOWLEDGMENTS

We are thankful for some financial assistance from the CSIR project (CSR-656-PHY), India.

[1] T. Matsui and H. Satz, *Phys. Lett. B* **178**, 416 (1986).
 [2] B. K. Patra, V. Agotiya, and V. Chandra, *Eur. Phys. J. C* **67**, 465 (2010).

[3] A. Mocsy and P. Petreczky, *Phys. Rev. D* **77**, 014501 (2008).

[4] A. Mocsy, *Eur. Phys. J. C* **61**, 705 (2009).

- [5] N. Brambilla, A. Pineda, J. Soto, and A. Vairo, *Nucl. Phys.* **B566**, 275 (2000).
- [6] N. Brambilla, A. Pineda, J. Soto, and A. Vairo, *Rev. Mod. Phys.* **77**, 1423 (2005).
- [7] W. E. Caswell and G. P. Lepage, *Phys. Lett.* **167B**, 437 (1986).
- [8] B. A. Thacker and G. P. Lepage, *Phys. Rev. D* **43**, 196 (1991).
- [9] G. T. Bodwin, E. Braaten, and G. P. Lepage, *Phys. Rev. D* **51**, 1125 (1995).
- [10] N. Brambilla, J. Ghiglieri, A. Vairo, and P. Petreczky, *Phys. Rev. D* **78**, 014017 (2008).
- [11] K. G. Wilson, *Phys. Rev. D* **10**, 2445 (1974).
- [12] Y. Makeenko, *Phys. At. Nucl.* **73**, 878 (2010).
- [13] J. Berges, Sz. Borsanyi, D. Sexty, and I.-O. Stamatescu, *Phys. Rev. D* **75**, 045007 (2007).
- [14] A. Barchielli, E. Montaldi, and G. M. Prospero, *Nucl. Phys.* **B296**, 625 (1988).
- [15] A. Rothkopf, *Mod. Phys. Lett. A* **28**, 1330005 (2013).
- [16] M. Laine, O. Philipsen, P. Romatschke, and M. Tassler, *J. High Energy Phys.* **03** (2007) 054.
- [17] A. Beraudo, J. P. Blaizot, and C. Ratti, *Nucl. Phys.* **A806**, 312 (2008).
- [18] F. Karsch, M. G. Mustafa, and M. H. Thoma, *Phys. Lett. B* **497**, 249 (2001).
- [19] A. Mocsy and P. Petreczky, *Eur. Phys. J. C* **43**, 77 (2005).
- [20] C.-Y. Wong, *Phys. Rev. C* **72**, 034906 (2005).
- [21] A. Mocsy and P. Petreczky, *Phys. Rev. D* **73**, 074007 (2006).
- [22] D. Cabrera and R. Rapp, *Phys. Rev. D* **76**, 114506 (2007).
- [23] A. Mocsy and P. Petreczky, *Phys. Rev. Lett.* **99**, 211602 (2007).
- [24] W. M. Alberico, A. Beraudo, A. De Pace, and A. Molinari, *Phys. Rev. D* **77**, 017502 (2008).
- [25] A. Mocsy and P. Petreczky, *Phys. Rev. D* **77**, 014501 (2008).
- [26] Ph. de Forcrand, M. Pérez, T. Hashimoto, S. Hioki, H. Matsufuru, O. Miyamura, A. Nakamura, I.-O. Stamatescu, T. Takaishi, and T. Umeda, *Phys. Rev. D* **63**, 054501 (2001).
- [27] B. K. Patra and D. K. Srivastava, *Phys. Lett. B* **505**, 113 (2001). D. Pal, B. K. Patra, and D. K. Srivastava, *Eur. Phys. J. C* **17**, 179 (2000).
- [28] B. K. Patra and V. J. Menon, *Eur. Phys. J. C* **48**, 207 (2006); **44567** (2005); **37115** (2004); *Nucl. Phys.* **A708**, 353 (2002).
- [29] B. Schenke and M. Strickland, *Phys. Rev. D* **76**, 025023 (2007).
- [30] M. Martinez and M. Strickland, *Phys. Rev. Lett.* **100**, 102301 (2008); M. Martinez and M. Strickland, *Phys. Rev. C* **78**, 034917 (2008).
- [31] Y. Burnier, M. Laine, and M. Vepsalainen, *J. High Energy Phys.* **01** (2008) 043.
- [32] M. Laine, O. Philipsen, and M. Tassler, *J. High Energy Phys.* **09** (2007) 066; T. Hatsuda, *Nucl. Phys.* **A904**, 210c (2013).
- [33] P. Petreczky, C. Miao, and A. Mocsy, *Nucl. Phys.* **A855**, 125 (2011).
- [34] N. Brambilla, M. A. Escobedo, J. Ghiglieri, J. Soto, and A. Vairo, *J. High Energy Phys.* **09** (2010) 038.
- [35] M. A. Escobedo, J. Soto, and M. Mannarelli, *Phys. Rev. D* **84**, 016008 (2011).
- [36] L. Grandchamp, S. Lumpkins, D. Sun, H. van Hees, and R. Rapp, *Phys. Rev. C* **73**, 064906 (2006).
- [37] R. Rapp, D. Blaschke, and P. Crochet, *Prog. Part. Nucl. Phys.* **65**, 209 (2010).
- [38] F. Riek and R. Rapp, *New J. Phys.* **13**, 045007 (2011).
- [39] A. Emerick, X. Zhao, and R. Rapp, *Eur. Phys. J. A* **48**, 72 (2012).
- [40] X. Zhao and R. Rapp, *Nucl. Phys.* **A859**, 114 (2011).
- [41] Y. Akamatsu and A. Rothkopf, *Phys. Rev. D* **85**, 105011 (2012).
- [42] M. Strickland and D. Bazow, *Nucl. Phys.* **A879**, 25 (2012).
- [43] A. Rothkopf, T. Hatsuda, and S. Sasaki, *Proc. Sci., LAT2009* (2009) 162; A. Rothkopf, T. Hatsuda, and S. Sasaki, *Phys. Rev. Lett.* **108**, 162001 (2012).
- [44] Y. Burnier and A. Rothkopf, *Phys. Rev. D* **86**, 051503 (2012).
- [45] B. Beinlich, F. Karsch, E. Laermann, and A. Peikert, *Eur. Phys. J. C* **6**, 133 (1999).
- [46] F. Karsch, E. Laermann, and A. Peikert, *Phys. Lett. B* **478**, 447 (2000).
- [47] Y. Aoki, G. Endrodi, Z. Fodor, S. D. Katz, and K. K. Szabo, *Nature (London)* **443**, 675 (2006).
- [48] F. Karsch, *J. Phys. Conf. Ser.* **46**, 122 (2006).
- [49] M. Cheng *et al.*, *Phys. Rev. D* **78**, 034506 (2008).
- [50] Y. Maezawa, N. Ukita, S. Aoki, S. Ejiri, T. Hatsuda, N. Ishii, and K. Kanaya, *Phys. Rev. D* **75**, 074501 (2007).
- [51] Oleg Andreev and Valentine I. Zakharov, *Phys. Lett. B* **645**, 437 (2007).
- [52] Vijai V. Dixit, *Mod. Phys. Lett. A* **05**, 227 (1990).
- [53] Helmut Satz, *J. Phys. G* **32**, R25 (2006).
- [54] V. Agotiya, V. Chandra, and B. K. Patra, *Phys. Rev. C* **80**, 025210 (2009).
- [55] V. Agotiya, V. Chandra, and B. K. Patra, arXiv:0910.0586.
- [56] P. Romatschke and M. Strickland, *Phys. Rev. D* **68**, 036004 (2003).
- [57] A. Dumitru, Y. Guo, and M. Strickland, *Phys. Lett. B* **662**, 37 (2008).
- [58] A. Dumitru, Y. Guo, A. Mocsy, and M. Strickland, *Phys. Rev. D* **79**, 054019 (2009).
- [59] Y. Burnier, M. Laine, and M. Vepsalainen, *Phys. Lett. B* **678**, 86 (2009).
- [60] A. Dumitru, Y. Guo, and M. Strickland, *Phys. Rev. D* **79**, 114003 (2009).
- [61] M. Margotta, K. McCarty, C. McGahan, M. Strickland, and D. Y. Elorriaga, *Phys. Rev. D* **83**, 105019 (2011).
- [62] L. Thakur, N. Haque, U. Kakade, and B. K. Patra, *Phys. Rev. D* **88**, 054022 (2013).
- [63] M. A. Escobedo and J. Soto, *Phys. Rev. A* **78**, 032520 (2008).
- [64] M. Laine, *Nucl. Phys.* **A820**, 25c (2009).
- [65] A. Dumitru, Y. Guo, and M. Strickland, *Phys. Rev. D* **79**, 114003 (2009).
- [66] S. Digal, O. Kaczmarek, F. Karsch, and H. Satz, *Eur. Phys. J. C* **43**, 71 (2005).
- [67] E. Megias, E. Ruiz Arriola, and L. L. Salcedo, *Indian J. Phys.* **85**, 1191 (2011).

- [68] E. Megias, E. Ruiz Arriola, and L. L. Salcedo, *Phys. Rev. D* **75**, 105019 (2007).
- [69] M. H. Thoma, [arXiv:hep-ph/0010164](https://arxiv.org/abs/hep-ph/0010164).
- [70] E. Braaten and R. D. Pisarski, *Nucl. Phys.* **B337**, 569 (1990).
- [71] P. F. Kelly, Q. Liu, C. Lucchesi, and C. Manuel, *Phys. Rev. D* **50**, 4209 (1994).
- [72] J. -P. Blaizot and E. Iancu, *Nucl. Phys.* **B417**, 608 (1994).
- [73] M. E. Carrington, H. Defu, and M. H. Thoma, *Eur. Phys. J. C* **7**, 347 (1999); *Phys. Rev. D* **58**, 085025 (1998).
- [74] M. Martinez and M. Strickland, *Phys. Rev. C* **79**, 044903 (2009).
- [75] A. Schneider, *Phys. Rev. D* **66**, 036003 (2002).
- [76] H. A. Weldon, *Phys. Rev. D* **26**, 1394 (1982).
- [77] J. I. Kapusta and C. Gale, *Finite Temperature Field Theory Principle and Applications* (Cambridge University Press, Cambridge, 1996), 2nd ed.
- [78] J. -P. Blaizot and E. Iancu, *Phys. Rep.* **359**, 355 (2002).
- [79] K. Kajantie, M. Laine, J. Peisa, A. Rajantie, K. Rummukainen, and M. E. Shaposhnikov, *Phys. Rev. Lett.* **79**, 3130 (1997).
- [80] P. Petreczky, *Eur. Phys. J. C* **43**, 51 (2005).
- [81] A. Dumitru, *Prog. Theor. Phys. Suppl.* **187**, 87 (2011).
- [82] M. Martinez and M. Strickland, *Nucl. Phys.* **A856**, 68 (2011).
- [83] R. Ryblewski and W. Florkowski, *J. Phys. G* **38**, 015104 (2011).
- [84] O. Philipsen and M. Tassler, [arXiv:0908.1746](https://arxiv.org/abs/0908.1746).
- [85] A. Dumitru, Y. Guo, A. Mocsy, and M. Strickland, *Phys. Rev. D* **79**, 054019 (2009).